PROCEEDINGS OF SCIENCE

Performance studies of LHCf and ATLAS-ZDC for very forward neutron measurement

Haruka Kobayashi[a,*] **and for the LHCf collaboration and ATLAS collaboration**

[a] *Institute for Space-Earth Environmental Research, Nagoya University, Nagoya, Japan*

E-mail: kobayashi.haruka.m7@s.mail.nagoya-u.ac.jp

It is important to understand hadronic interactions for the indirect measurement of high energy cosmic rays that are E> 10^{15} eV. Large Hadron Collider forward (LHCf) and ATLAS Zero Degree Calorimeter (ZDC) measure neutral particles generated in the very forward region of pp collisions at LHC. The LHCf detector is a calorimeter that has a thickness of 1.7 interaction lengths, resulting in large hadronic shower particle leakage. To address this, the combined analysis with ATLAS-ZDC which is installed behind the LHCf and has a thickness of 3.4 interaction lengths, enables an improvement in the energy resolution of hadronic particles from 40% to 20%, which was confirmed with 350 GeV proton beam at SPS.

In 2022, we conducted the LHCf+ATLAS-ZDC joint operation with pp collision at $\sqrt{s}$=13.6 TeV. We evaluated the improvement in resolution for very forward neutron measurement using the operational data with joint analysis. Additionally, neutron trigger efficiency and particle identification (PID) efficiency were studied with Monte Carlo simulations.

39th International Cosmic Ray Conference (ICRC2025)
15–24 July 2025
Geneva, Switzerland

*Speaker

© Copyright owned by the author(s) under the terms of the Creative Commons Attribution-NonCommercial-NoDerivatives 4.0 International License (CC BY-NC-ND 4.0).

PoS(ICRC2025)303

1. Introduction

It is essential to understand hadronic interactions for high-energy cosmic-ray observations. Extensive air shower (EAS) measurements face the difficulty that the mass composition cannot be uniquely determined[1]. Mass composition is a crucial observable for investigating how and where high-energy cosmic rays are accelerated and how they propagate. This limitation arises from fluctuations in the predictions of hadronic interaction models.

The LHC-forward (LHCf) experiment measures forward neutral particles produced in pp collisions at the LHC in order to study hadronic interaction processes. The collisions at the current LHC energy, $\sqrt{s} = 13.6, \mathrm{TeV}$, correspond to those of $10^{17}, \mathrm{eV}$ cosmic rays interacting with atmospheric nuclei. The LHCf and ATLAS-Zero Degree Calorimeter (ZDC) detectors are located on both sides of the ATLAS interaction point, 140 m away, and measure neutral particles such as neutrons and photons. The LHCf detector covers the pseudorapidity region $|\eta| > 8.4$. A joint measurement with ATLAS-ZDC provides better neutron energy resolution than the LHCf measurement alone.

Very forward neutron measurement is interesting in terms of EAS observation. LHCf can detect the energetic neutrons that have TeV energy, and then we measure the inelasticity of the pp collision[2]. Inelasticity is very important for the air shower development and affect X_{max}[3]. We could also detect neutrons generated by the one-pion-exchange[4] or Λ decay. By one-pion-exchange, the measurement of proton and virtual pion interaction of $E_{\mathrm{lab}} = 15\,\mathrm{PeV}$ is expected, although $p - \pi$ measurement was carried out in low energy, $E_{\mathrm{lab}} = 350\,\mathrm{GeV}$, by the fixed target experiment until now. This will help us understand the high-energy $p - \pi$ interactions that occur many times in EAS. Forward Λ measurement will reveal whether the strange barions are enhanced in very forward region, this result might be connected with muon excess[5].

LHCf and ATLAS joint operation is performed in the pp collision of $\sqrt{s} = 13.6\,\mathrm{TeV}$ in September 2022 at LHC, exchanging the LHCf and ATLAS triggers. In this proceeding, we present the performance of LHCf and ATLAS-ZDC joint operation studied using the joint operation at LHC in 2022.

2. Setup of LHCf + ATLAS-ZDC measurement

2.1 LHCf detector and ATLAS-ZDC detector

LHCf has two detectors, Arm1 and Arm2 detector, on both sides of the interaction point. In this study, we only use LHCf Arm1 detector (Figure 1) and three ATLAS-ZDC hadronic modules (Figure 2).

The LHCf Arm1 detector consists of two calorimeters: the small tower (TS) and the large tower (TL). The thickness is 44 radiation length equivalent to 1.7 interaction length. Both TS and TL calorimeters have 16 layers of tungsten for energy absorption, 16 sampling layers of Gd_2SiO_5 (GSO) scintillator and 4 layers of GSO bar hodoscope for position detection at 6, 10, 32 and $42X_0$. The step of the sampling layers is $2X_0$ from 1st to 11th layer, $4X_0$ from 12th layer. The light from GSO scintillator is collected in the PMT placed above the calorimeter.

The ATLAS-ZDC detector consists of three calorimeter modules vertically aligned along the beam direction. Each module comprises 11 layers of tungsten absorbers and 12 layers of fused-silica

PoS(ICRC2025)303

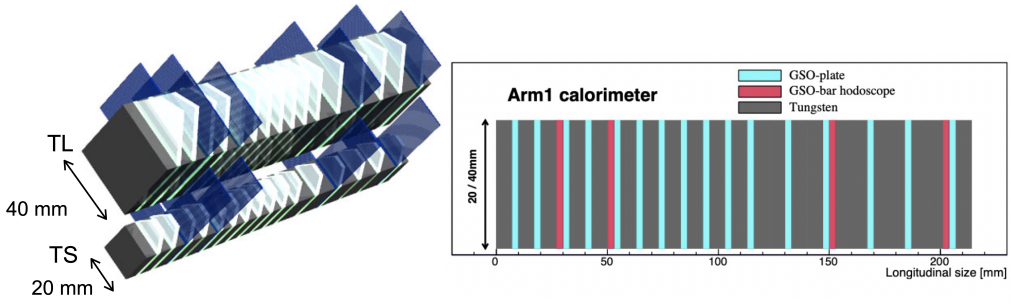

(a) (b)

Figure 1: The schematic view of LHCf arm1 calorimeter

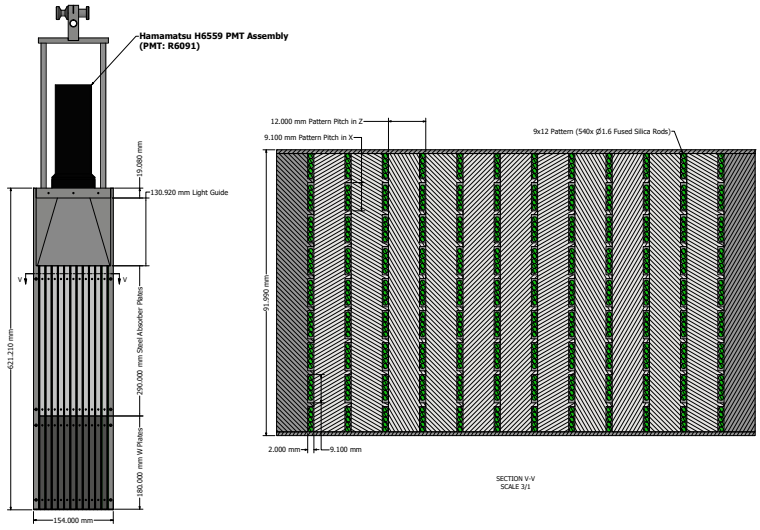

Figure 2

fibers, which transmit Cherenkov light to a photomultiplier tube (PMT) located at the top. Therefore, the ATLAS-ZDC measures the energy deposited in each module, but not the particle positions. The combined thickness of the three ATLAS-ZDC modules corresponds to 3.4 interaction lengths. The ATLAS-ZDC detectors are installed downstream of the LHCf detector. Hadronic showers initiated by neutrons can deposit energy in both the LHCf and ATLAS-ZDC detectors.

2.2 Joint operation setup in 2022

We conducted the LHCf+ATLAS joint operation with low-luminosity pp collision in $\sqrt{s}$ = 13.6 TeV at LHC from September 22nd to 26th in 2022 (Figure 3). The LHCf and ATLAS-ZDC detectors were installed at 140m from ATLAS interaction point and measured the neutral particles such as photons or neutrons in very forward region ($\eta > 8.8$). We realized joint data taking by exchanging each DAQ triggers. ATLAS recorded all LHCf triggered events. We obtained 165 million events in this operation. Event matching of LHCf and ATLAS data is taken after the operation.

PoS(ICRC2025)303

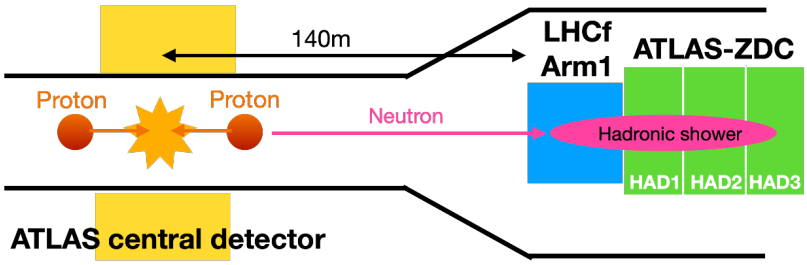

Figure 3

3. Energy reconstruction method

The hadronic particle energies are reconstructed by combining the energy deposits measured by LHCf and ATLAS-ZDC [6]. In this analysis, we use the LHCf energy deposit recorded by LHCf and the ATLAS-ZDC energy deposit recorded by ATLAS. Although LHCf also received and recorded analog signals of the three ATLAS-ZDC hadronic modules, these values exhibited larger fluctuations than the values recorded by ATLAS.

The correlation between energy deposition of LHCf and ATLAS-ZDC is anti-linear for hadronic particles at a given injection energy. Therefore, energy estimator is defined as

$$E_{\mathrm{est}} = \Delta E_{\mathrm{LHCf}} + \alpha \Delta E_{\mathrm{ZDC}} \tag{1}$$

where α represents scale factor which is defined from the slope of the correlation between ΔE_{LHCf} and ΔE_{ZDC} obtained by MC simulation horizontally injecting 3 TeV proton to LHCf detector. Then, reconstructed energy E_{rec} is estimated as

$$E_{\mathrm{rec}} = F(E_{\mathrm{est}}) \tag{2}$$

where F is quadratic function defined using MC simulation injecting protons with different energies.

The injected XY positions are defined by shower core position measured by GSO bar XY hodoscopes of LHCf Arm1 detector.

4. Performance of neutron identification with MC simulation

The selection criteria for neutrons use only LHCf information. We applied two types of conditions to select the neutron events, which are hadron trigger and neutron particle identification (PID) defined by character of hadronic shower development. We use EPICS and Cosmos simulation code [7] for LHCf detector simulation. We present the performance of these two neutron selection criteria.

Hadronic showers develop in the rear part of the LHCf calorimeter though the EM showers initialized by photons develop in the forward part of the calorimeter. Therefore, the hadron trigger is defined by an energy deposit greater than 0.6 GeV in three consecutive layers among layer 10th to 15th. Figure 4 shows the hadron trigger efficiency as a function of the true neutron energy, based on a MC simulation where neutrons are injected horizontally into the LHCf calorimeter. We observed that the trigger efficiency increases up to 4 TeV, after which it is constant about 0.7.

PoS(ICRC2025)303

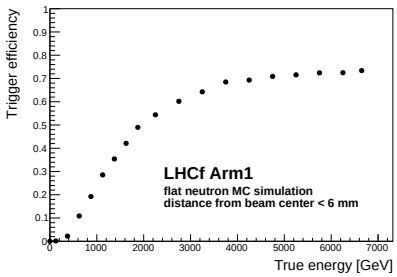

Figure 4: Hadron trigger efficiency as a function of true energy in the MC simulation

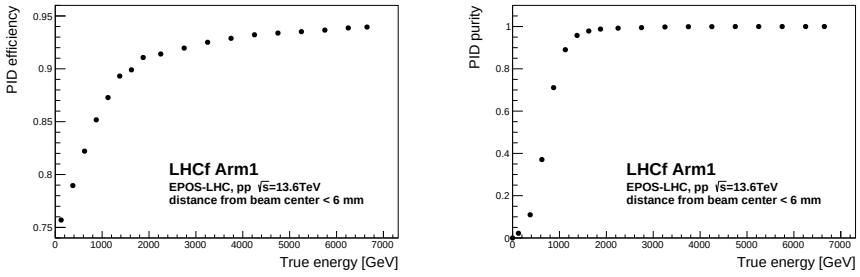

(a) (b)

Figure 5: Neutron PID efficiency and purity as a function of true energy in the MC simulation.

Neutron identification criteria based on shower development characteristics were also applied. We define

$$L_{2D} = L_{90} - 0.25 \cdot L_{20} \tag{3}$$

where L_{90} and L_{20} are the depths at which 90% and 20% of the total deposited energy are accumulated, respectively. We then require $L_{2D} > 20$ r.l. for neutron PID [8]. We used the MC simulation generated by EPOS-LHC for interaction model of pp collisions for obtaining the PID efficiency and purity. Figure 5(a) and Figure 5(b) show the neutron PID efficiency and purity respectively. The PID efficiency exceeds 0.9 above 2 TeV, and the purity approaches unity above 1.5 TeV.

5. Performance by joint analysis of operation performed in 2022

Data obtained in the low-luminosity special run with pp collisions at $\sqrt{s}$ =13.6 TeV in September 2022 is used for comparing the energy distibution of neutron-like events by LHCf standalone analysis method and LHCf+ATLAS-ZDC joint analysis method. We applied the neutron selection criteria using only the LHCf detector, as described in the previous section. Figure 6 shows the hit map of neutrons injected into the LHCf Arm1 TS calorimeter. The position is determined by the GSO bar XY hodoscopes of the LHCf Arm1 detector. Figure 6 shows that a lot of neutrons are injected to the region near the beam center. In this analysis, we selected events in which neutrons were incident within a 6 mm radius from the beam center, corresponding to the red circle in Figure 6.

PoS(ICRC2025)303

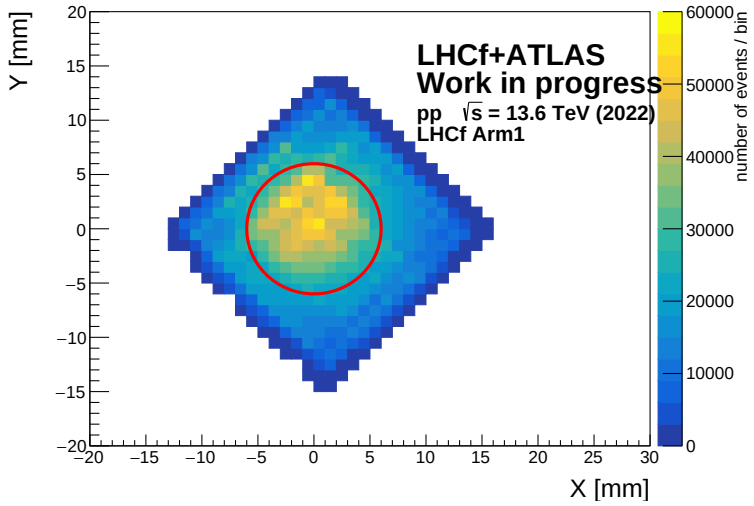

Figure 6: Hitmap of LHCf Arm1 small tower for neutron-like event. position is determined by LHCf detector. The xy axis shows the beam center coordinate. The point (0,0) is the beam center projected to the LHCf detector.

Figure 7 shows comparison of energy distribution by LHCf standalone reconstruction method and LHCf+ATLAS-ZDC combined reconstruction method. It is observed that the peaks of both energy distributions occur at the same energy, but the distribution becomes narrower in the joint analysis. The improvement in energy resolution achieved by the LHCf + ATLAS-ZDC analysis is evident when using the 2022 operation data.

6. Summary

The operation of pp collision ($\sqrt{s}$ = 13.6 TeV) with low luminosity at LHC was carried out in 2022 with LHCf+ATLAS joint data taking exchanging both DAQ triggers. We selected neutron-like events from operation data and confirmed the efficiency of neutron selection criteria by detector simulation. We confirmed that the neutron energy resolution was improved by the LHCf+ATLAS-ZDC joint analysis using real operation data. The improvement in neutron energy resolution allows us to proceed to the next step of measuring one-pion-exchange events, Λ^0, and all forward neutron events.

References

[1] A. Abdul Halim, P. Abreu, et al. Inference of the Mass Composition of Cosmic Rays with Energies from $10^{18.5}$ to 10^{20} eV Using the Pierre Auger Observatory and Deep Learning. *Phys. Rev. Lett.*, 134:021001, Jan 2025. doi:10.1103/PhysRevLett.134.021001.

[2] O. Adriani, E. Berti, et al. Measurement of energy flow, cross section and average inelasticity of forward neutrons produced in $\sqrt{s}$ = 13 TeV proton-proton collisions with the LHCf Arm2 detector. *Journal of High Energy Physics*, 2020(7), July 2020. doi:10.1007/jhep07(2020)016.

PoS(ICRC2025)303

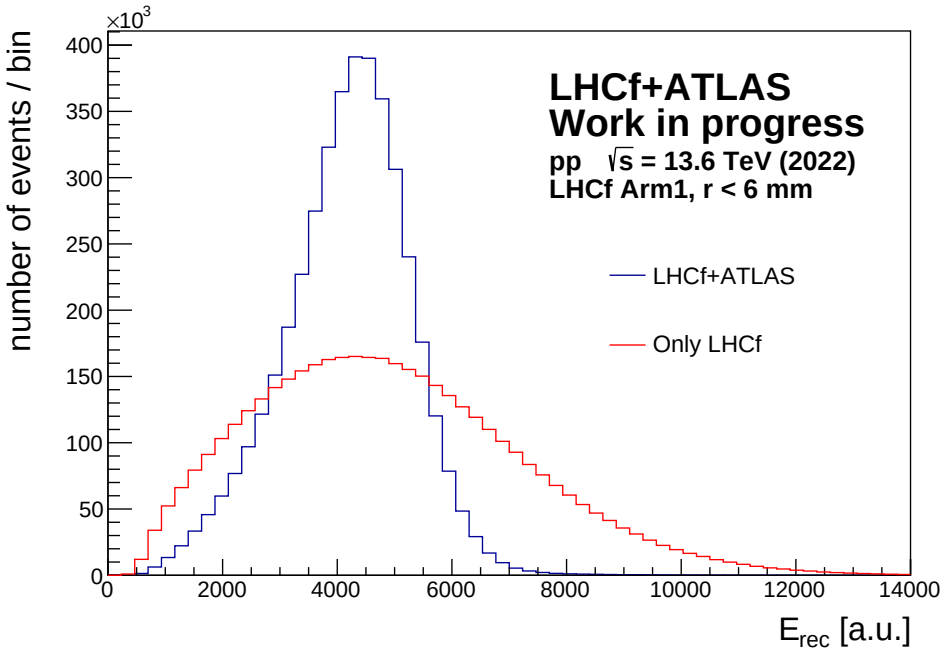

Figure 7: Comparison between neutron reconstructed energy distribution by LHCf+ATLAS-ZDC joint analysis method and LHCf standalone method.

[3] Ralf Ulrich, Ralph Engel, and Michael Unger. Hadronic multiparticle production at ultrahigh energies and extensive air showers. *Physical Review D*, 83(5), March 2011. doi:10.1103/physrevd.83.054026.

[4] R. A. Ryutin. Total pion–proton cross section from the new lhcf data on leading neutrons spectra. *The European Physical Journal C*, 77(2), February 2017. doi:10.1140/epjc/s10052-017-4690-3.

[5] Johannes Albrecht et al. The Muon Puzzle in cosmic-ray induced air showers and its connection to the Large Hadron Collider. *Astrophysics and Space Science*, 367(3), March 2022. doi:10.1007/s10509-022-04054-5.

[6] Kobayashi, Haruka. Performance of hadronic shower measurement with lhcf and atlas zdc detectors. *EPJ Web Conf.*, 320:00043, 2025. doi:10.1051/epjconf/202532000043.

[7] K. Kasahara. Epics web page. URL: https://cosmos.n.kanagawa-u.ac.jp.

[8] O. Adriani, E. Berti, et al. Measurement of inclusive forward neutron production cross section in proton-proton collisions at $\sqrt{s}$ = 13 TeV with the LHCf Arm2 detector. *Journal of High Energy Physics*, 2018(11), November 2018. doi:10.1007/jhep11(2018)073.

PoS(ICRC2025)303